

NONLINEAR BENDING OF BIMODULAR-MATERIAL PLATES

J. N. REDDY and W. C. CHAO

Department of Engineering Science and Mechanics, Virginia Polytechnic Institute and State University,
Blacksburg, VA 24061, U.S.A.

(Received 11 January 1982; received for publication 17 May 1982)

Abstract—The paper presents finite element results for geometrically nonlinear bending of fiber-reinforced, single-layer and two-layer cross-ply rectangular plates constructed of materials which have linear elastic properties in tension and compression that are different. A shear deformation theory of layered composite plates, accounting for large rotations (in the von Karman sense) and the bimodular action, is employed to analyze rectangular plates made of two cord-rubber bimodular materials. Numerical results for transverse deflection are presented for simply supported plates under sinusoidally distributed and uniformly distributed transverse loads.

INTRODUCTION

The present paper is a continuation of the research by the authors and their colleagues [1-5] in the analysis of bimodular composite plates. The previous investigations by the authors and others were based on geometrically linear theory of plates. The only exception to this statement is provided by the works of Kamiya [6, 7], which are concerned with a clamped circular plate, and a simply supported rectangular plate under sinusoidally distributed load, respectively. The present paper employs the finite element developed in [2, 8] and the fiber-governed constitutive model of Bert [9] to investigate the geometrically nonlinear response of bimodular-material plates. The following brief review of literature provides a background for the present paper.

Analysis of plates made of bimodular materials began with the work of Ambartsumyan [10] in 1965 (although Timoshenko [11] considered the flexural stresses in such materials as early as 1941, Ambartsumyan's work is credited for the renewed interest in the analysis of bimodular materials). Shapiro [12] considered the simple problem of a circular plate under a pure bending moment at its edge. Kamiya [6, 7] analyzed the large-deflection behavior of clamped circular plates using a finite difference technique, and rectangular plates under sinusoidally distributed load using the Galerkin method. In these investigations, only bimodular isotropic materials were considered, and the transverse shear strains were omitted. The effect of thickness shear deformation was included in the simple case of cylindrical bending by Kamiya [13]. The first analysis of bimodular, anisotropic materials is apparently due to Jones and Morgan [14], who treated cylindrical bending of a thin, cross-ply laminate. In the last couple of years, a number of papers dealing with the static bending and free vibration of single-layer and two-layer cross-ply plates have appeared [1-5, 15-17]. Most of these works are a result of the support of the research by C. W. Bert at the University of Oklahoma and the senior author by the Office of Naval Research. The significant contributions of this research over previous works are:

- (i) The material of each layer is both elastically and thermoelastically orthotropic and bimodular;
- (ii) Both single-layer orthotropic and two-layer cross-ply laminated plate and shell constructions were considered using a fibre-governed constitutive model;
- (iii) Transverse shear strains are included;
- (iv) Simply-supported and clamped boundary conditions are considered, and sinusoidal distribution as well as uniform distribution of transverse load and temperature changes are considered;
- (v) Static, transient, and free vibration responses are studied;
- (vi) Both exact (for certain edge conditions and loadings) and finite-element analyses are presented.

The present paper investigates the large-deflection (in the von Karman sense) behavior of single-layer orthotropic and two-layer cross-ply plates.

2. GOVERNING EQUATIONS

Consider a plate constructed of a finite number of uniform-thickness, orthotropic, bimodular-material layers oriented arbitrarily with respect to the plate axes. The plate coordinates are taken such that the xy -plane coincides with the midplane of the plate. Under the assumptions that the layers remain linearly elastic during the deformation and the generalized Hooke's law is valid, and that no debonding occurs between layers, one can employ the equations governing the shear deformable theory of layered composite plates [8, 18]. Since these equations are amply documented in the works cited earlier (see, e.g. [1-5]), only the strain-displacement relations and the equations of motion will be repeated here to indicate the nonlinear terms resulting from the von Karman theory.

Assuming that the conditions of the von Karman plate theory are valid, and accounting for the transverse shear strains, the strain-displacement relations can be expressed in the form,

$$\begin{aligned}\epsilon_1 &= \frac{\partial u}{\partial x} + \frac{1}{2} \left(\frac{\partial w}{\partial x} \right)^2 + z \frac{\partial \psi_x}{\partial x} \equiv \epsilon_1^0 + z\kappa_1 \\ \epsilon_2 &= \frac{\partial v}{\partial y} + \frac{1}{2} \left(\frac{\partial w}{\partial y} \right)^2 + z \frac{\partial \psi_y}{\partial y} \equiv \epsilon_2^0 + z\kappa_2 \\ \epsilon_6 &= \frac{\partial u}{\partial y} + \frac{\partial v}{\partial x} + \frac{\partial w}{\partial x} \frac{\partial w}{\partial y} + z \left(\frac{\partial \psi_x}{\partial y} + \frac{\partial \psi_y}{\partial x} \right) \equiv \epsilon_6^0 + z\kappa_6 \\ \epsilon_5 &= \psi_x + \frac{\partial w}{\partial x}, \quad \epsilon_4 = \psi_y + \frac{\partial w}{\partial y}.\end{aligned}\tag{2.1}$$

Here u , v , w are the midplane displacements along x , y , z directions; and ψ_x and ψ_y are the slopes in the xz and yz planes due to bending only. In writing the strain-displacement equations, it is assumed that the products of ψ_x , ψ_y , $\partial u/\partial x$ and $\partial v/\partial y$ are negligible. Since the constitutive relations are based on the plane-stress assumption, strain ϵ_3 does not come into the equations.

Neglecting the body moments and surface shearing forces, the equations of equilibrium (in the absence of surface and body forces) can be written as,

$$\begin{aligned}N_{1,x} + N_{6,y} &= 0 \\ N_{6,x} + N_{2,y} &= 0 \\ Q_{1,x} + Q_{2,y} + N(N_i, w) &= q_0 \\ M_{1,x} + M_{6,y} - Q_1 &= 0 \\ M_{6,x} + M_{2,y} - Q_2 &= 0\end{aligned}\tag{2.2}$$

where N_i , Q_i , and M_i are the stress and moment resultants defined by

$$N(N_i, w) = \int_{-h/2}^{h/2} (1, z) \sigma_i dz, \quad (Q_1, Q_2) = \int_{-h/2}^{h/2} (\sigma_5, \sigma_4) dz,\tag{2.3}$$

and $N(\cdot)$ is the nonlinear operator,

$$N(N_i, w) = \frac{\partial}{\partial x} \left(N_1 \frac{\partial w}{\partial x} \right) + \frac{\partial}{\partial y} \left(N_6 \frac{\partial w}{\partial x} \right) + \frac{\partial}{\partial x} \left(N_6 \frac{\partial w}{\partial y} \right) + \frac{\partial}{\partial y} \left(N_2 \frac{\partial w}{\partial y} \right).\tag{2.4}$$

Here σ_i ($i = 1, 2, 4, 5, 6$) denote the stress components ($\sigma_1 = \sigma_x$, $\sigma_2 = \sigma_y$, $\sigma_4 = \sigma_{yz}$, $\sigma_5 = \sigma_{xz}$ and $\sigma_6 = \sigma_{xy}$).

3. FINITE-ELEMENT FORMULATION

The finite-element model used in the present study is the same as that employed in [2] except for the inclusion of the nonlinear terms. The formulation is not repeated here but the

steps involved in the nonlinear analysis of the bimodular-material plates are pointed out. The finite-element model, for a typical element, in the present case is of the following form

$$[K]\{\Delta\} = \{F\}, \quad (3.1)$$

where $\{\Delta\}$ denotes the column of the nodal values of the generalized displacements. The elements of the element stiffness matrix $[K]$ are given in Appendix 1.

Several comments are in order on the computational scheme used in the present study. First one should note that the stiffness matrix $[K]$ is nonlinear in that it depends on the displacement vector. Therefore, an iteration technique must be used. On the other hand, the calculation of the stiffness coefficients requires the knowledge of the neutral surface locations,

$$\begin{aligned} z_{nx} &= - \left[u_{,x} + \frac{1}{2}(w_{,x})^2 \right] / \psi_{x,x} \\ z_{ny} &= - \left[v_{,y} + \frac{1}{2}(w_{,y})^2 \right] / \psi_{y,y} \end{aligned} \quad (3.2)$$

which in turn depend on the solution $(u, v, w, \psi_x, \psi_y)$. Thus another iterative scheme is required for the determination of the neutral surface locations. The latter iterative scheme begins with assumed values of z_{nx} and z_{ny} (say, $z_{nx} = z_{ny} = 0$) and then A_{ij} , B_{ij} and D_{ij} are computed using these values. In general, the neutral-surface locations are not independent of the position (x, y) , and therefore, the expressions for plate stiffnesses, A_{ij} , B_{ij} and D_{ij} , also depend on x and y coordinates. Since the element stiffness coefficients K_{ij} are evaluated at the Gauss points, the plate stiffnesses A_{ij} , B_{ij} and D_{ij} are also evaluated at the Gauss points by using the neutral-surface positions computed at the Gauss points. After obtaining the generalized displacements, the neutral-surface locations are recomputed. Using these new values of z_{nx} and z_{ny} , the stiffnesses for the next iteration are computed. This procedure is repeated until the difference between any two consecutive values of z_{nx} (and z_{ny}) differ by a small preselected value (say 0.1%). Once the convergence on the neutral surface locations is achieved, iteration on the nonlinear stiffnesses is carried until convergence on the displacements is achieved.

4. NUMERICAL RESULTS AND DISCUSSION

In the following, numerical results are presented for rectangular plates made of two bimodular materials: aramid cord-rubber (AR) and polyester cord-rubber (PR), which are used in automobile tires. The material properties for these two materials are given in Table 1. In the present study, a 2×2 mesh of nine-node isoparametric elements in the quarter plate was used. The shear correction coefficients k_s^2 were chosen to be $5/6$. All of the computations were carried on an IBM 3032 computer in double precision.

A summary of the linear analysis is presented in Table 2. The effect of the aspect ratio (b/a) and thickness-to-side ratio (h/a) on nondimensionalized center deflection (\bar{w}) is apparent from the results in Table 2 (also see Figs. 1 and 2). The effect of the transverse shear deformation is to increase the nondimensionalized center deflection as much as 30% for a side-to-thickness ratio of $a/h = 25$.

The results of geometrically nonlinear bending of bimodular plates are discussed next. In order to validate the present element for the nonlinear analysis, first, single-layer and two-layer

Table 1. Material properties for aramid cord-rubber and polyester cord-rubber, unidirectional, bimodulus composite materials

Property	Aramid-Rubber		Polyester-Rubber	
	Tensile	Compressive	Tensile	Compressive
E_{11} (GPa)	3.58	0.012	0.617	0.0369
E_{22} (GPa)	0.00909	0.012	0.008	0.0106
ν_{12}	0.416	0.205	0.475	0.185
$G_{12} = G_{13}$ (GPa)	0.0037	0.0037	0.00262	0.00267
G_{23} (GPa)	0.0029	0.00499	0.00233	0.00475

Table 2. Comparison of closed-form and finite element solutions of single-layer (0°) and two-layer (0°/90°) rectangular plates of aramid-rubber material (linear analysis)

b/a	h/a	single-layer (0°)				Two-layer (0°/90°)			
		z_{nx}/h		\bar{w}^\dagger		z_{nx}/h		\bar{w}^\dagger	
		CFS	FES	CFS	FES	CFS	FES	CFS	FES
	CPT	0.4317	-	0.7124	-	0.4281	-	0.6960	-
0.6	0.01	0.4317	0.4316	0.7134	0.7137	0.4281	0.4280	0.6969	0.6973
	0.1	0.4318	0.4315	0.8134	0.8138	0.4282	0.4279	0.7830	0.7834
	0.2	0.4319	0.4316	1.1125	1.1128	0.4284	0.4281	1.0342	1.0345
	0.4	0.4322	0.4319	2.2862	2.2862	0.4290	0.4287	1.9802	1.9800
	0.5	0.4323	0.4320	3.1590	3.1589	0.4293	0.4289	2.6695	2.6689
	CPT	0.4420	-	1.8671	-	0.4383	-	1.7734	-
1.0	0.01	0.4420	0.4420	1.8689	1.8698	0.4383	0.4383	1.7751	1.7760
	0.1	0.4420	0.4417	2.0537	2.0546	0.4384	0.4381	1.9492	1.9502
	0.2	0.4421	0.4418	2.6058	2.6069	0.4385	0.4381	2.4635	2.4647
	0.4	0.4422	0.4419	4.7490	4.7504	0.4388	0.4384	4.3960	4.3976
	0.5	0.4423	0.4420	6.3228	6.3243	0.4389	0.4386	5.7764	5.7782
	CPT	0.4454	-	3.0096	-	0.4434	-	2.8916	-
2.0	.01	0.4454	0.4454	3.0123	3.0135	0.4434	0.4434	2.8941	2.8954
	0.1	0.4454	0.4452	3.2774	3.2783	0.4434	0.4431	3.1478	3.1490
	0.2	0.4454	0.4451	4.0774	4.0773	0.4434	0.4431	3.9130	3.9137
	0.4	0.4454	0.4451	7.2381	7.2337	0.4435	0.4431	6.9234	6.9220
	0.5	0.4455	0.4451	9.5801	9.5724	0.4435	0.4431	9.1397	9.1365

$$\dagger \bar{w} = (wE_2^c h^3) 10^2 / (q_0 a^4)$$

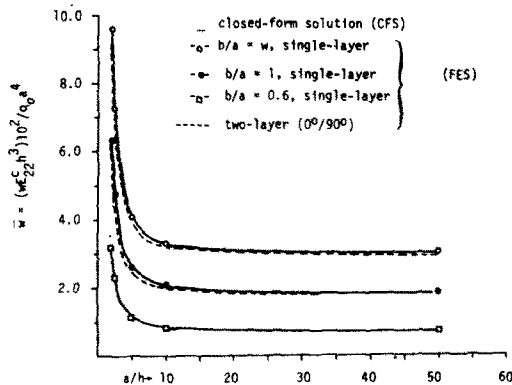


Fig. 1. Effect of side-to-thickness ratio (a/h) on the nondimensionalized deflection (\bar{w}) of single-layer (0°) and two-layer (0°/90°) rectangular plates of aramid-rubber bimodular material (small-deflection theory).

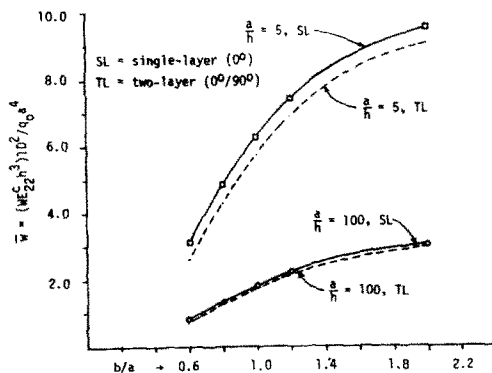


Fig. 2. Effect of aspect ratio (b/a) on the nondimensionalized deflection (\bar{w}) of single-layer (0°) and two-layer (0°/90°) rectangular plates of aramid-rubber bimodular material (small-deflection theory).

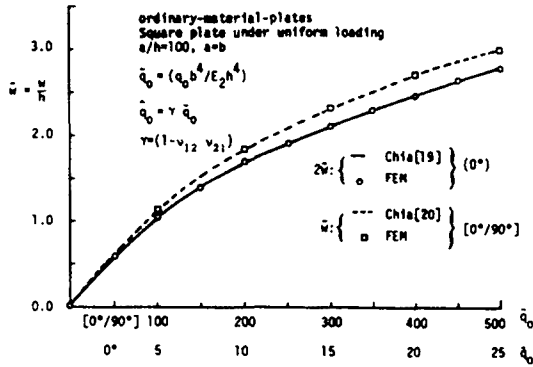


Fig. 3. Nonlinear center deflection of single- and two-layer cross-ply square plates under uniform loading ($E'_i = E^c$, $i = 1, 2$; simply supported boundary conditions).

cross-ply rectangular (ordinary, *not* bimodular) plates under uniformly distributed loading and simply supported boundary conditions were analyzed, and the results are compared with the analytical (perturbation) results of Chia [19, 20] in Fig. 3. The material properties of the single-layer plate ($a/h = 100$, $a/b = 1$) are (see [19])

$$E_1/E_2 = 20.0, G_{12}/E_2 = 0.5, \nu_{12} = 0.2. \tag{4.1}$$

The layer properties of the two-layer plate ($a/h = 100$, $a/b = 1$) are (see [20])

$$E_1/E_2 = 40.0, G_{12}/E_2 = 0.6, \nu_6 = 0.2. \tag{4.2}$$

The present results are in excellent agreement with those of Chia [19, 20]. Next, an isotropic, bimodular, simply supported square plate under sinusoidally distributed loading was analyzed in an effort to make comparisons with the results of Kamiya [7]. The present results are compared with those of Kamiya in Fig. 4. The present results do not agree with those of Kamiya [7] for all ratios of E^c/E' (including 1). Since our results are validated for $E^c/E' = 1$ in the previous example, one must come to the conclusion that Kamiya's [7] results are in error.

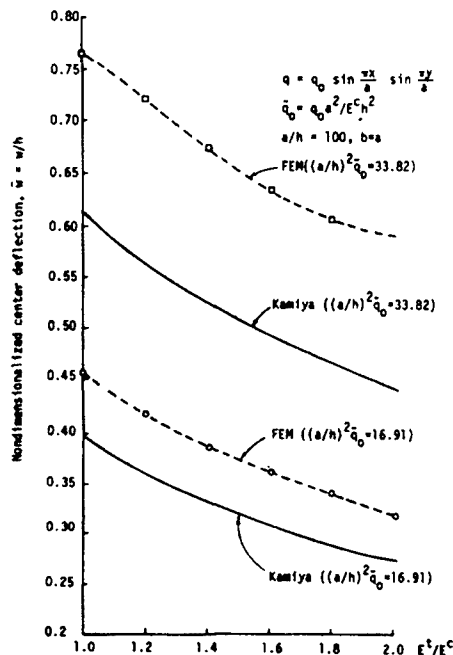


Fig. 4. Nondimensionalized center deflection versus the ratio of longitudinal modulus in tension to the longitudinal modulus in compression for an isotropic bimodular, square plate under sinusoidal loading (simply supported case).

Table 3. Nondimensionalized transverse deflection of single-layer (0°) and two-layer (0°/90°) square plates of aramid-rubber and polyester-rubber materials. ($a/h = 100$, $\bar{w} = w/h$, $\bar{q} = q_0 E_{22}^c a^4/h^4$)

\bar{q}	Aramid-Rubber			Polyester-Rubber		
	single-layer (0°)		0°/90°	single-layer (0°)		0°/90°
	SL	UDL	SL	SL	UDL	SL
Linear	0.1869	0.2959	0.1777	0.1081	0.1683	0.1776
10	0.1776	0.2720	0.1660	0.1069	0.1654	0.1707
20	0.3350	0.4963	0.3100	0.2110	0.3233	0.3254
30	0.4743	0.6821	0.4353	0.3115	0.4718	0.4639
40	0.5977	0.8417	0.5452	0.4081	0.6106	0.5879
50	0.7083	0.9798	0.6443	0.5006	0.7399	0.6997

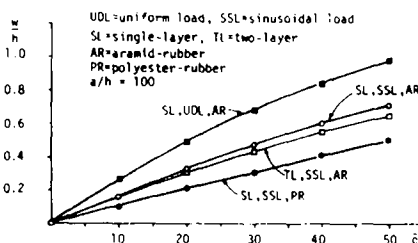


Fig. 5. Load-deflection curves for thin square plates of bimodular materials ($a/h = 100$).

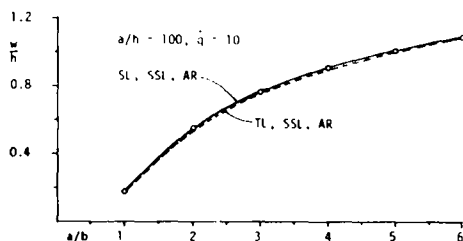


Fig. 6. Effect of plate aspect ratio on the nonlinear deflection of aramid-rubber bimodular-material rectangular plates under sinusoidal loading (SSL) (SL = single-layer, TL = two-layer, AR = aramid-rubber, PR = polyester-rubber).

The nondimensionalized center deflection (w/h) versus the load parameter ($\bar{q} = q_0 E_{22}^c a^4/h^4$) are presented in Table 3 for single-layer (0°) and two-layer (0°/90°) square plates ($a/h = 100$) aramid-rubber and polyester-rubber materials under sinusoidal loading and uniform loading. First note that the response of aramid-rubber plates is more nonlinear than that of polyester-rubber plates. Also note that the deflection due to uniform loading is about one and one-half times that due to sinusoidal loading (also see Fig. 5).

Plot of nondimensionalized center deflection versus the aspect ratio (a/b) is shown in Fig. 6 for single-layer and two-layer (0°/90°) aramid-rubber plates ($a/h = 100$) under sinusoidal loading (for the load parameter value of 10). The effect of the aspect ratio is, relatively, more pronounced in the two-layer plates than in the single-layer plates (the effect is to increase the deflection, $\bar{w} = w/h$).

Plots of the nondimensionalized center deflection versus the side-to-thickness ratio and the load parameter are shown, respectively, in Figs. 7 and 8 for aramid-rubber square plates under sinusoidal loading. From the plots presented in Fig. 7 it is clear that the effect of shear deformation is more pronounced with increasing values of the load parameter. This can also be seen from the load-deflection curves presented in Fig. 8.

5. SUMMARY AND CONCLUSIONS

Results of the finite-element analysis of the equations governing the Timoshenko-type shear deformable theory that accounts for geometric nonlinearities of the von Karman plate theory are presented for aramid-rubber and polyester-rubber bimodular composite plates under transverse loading. Both single-layer and two-layer cross-ply plates are analyzed under sinusoidally

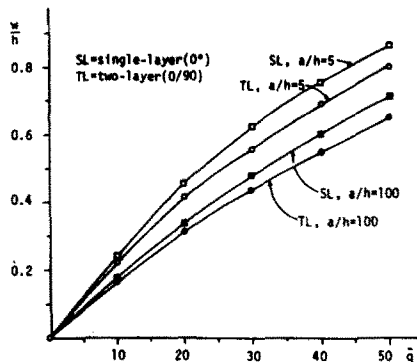


Fig. 7. Load-deflection curves for square plates of aramid-rubber bimodular material under sinusoidal loading.

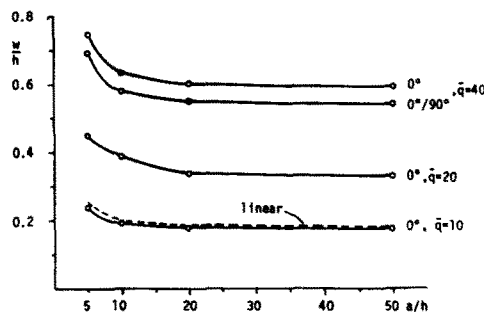


Fig. 8. Effect of side-to-thickness ratio on the nonlinear deflection (w/h) of square plates of aramid-rubber bimodular material ($a/h = 100$).

and uniformly distributed loads. The effect of the thickness-shear (which is to increase the deflection w/h with increasing values of side-to-thickness ratio, a/h) is more apparent for side-to-thickness ratios smaller than twenty, and for larger load parameter values. The finite-element analysis of ordinary—(i.e. not bimodular—) material plates whose elastic properties are taken to be the average of compressive and tensile properties listed in Table 1 show that the deflections predicted are about one-fourth (for aramid-rubber plates with $a/h = 10$) of those predicted using the bimodular properties (see [16]). Thus the effect of bimodularity is significant on the response.

As pointed out in the introduction of this paper, there is only a little to be done in the way of finite-element analyses of bimodular plates. The nonlinear transient response of bimodular plates seems to be the final step in the series of investigations based on the fiber-governed constitutive model. As far as the constitutive models are concerned, there is still a need for improved and/or realistic models. If a single functional relationship between stresses and strains were available for both compressive and tensile regions, the analysis would be much cleaner (free of any assumption concerning the state of stress or strain in the material).

Acknowledgements—The support of the research reported herein by the Mechanics Division of the Office of Naval Research through Contract N00014-78-C-0647 is gratefully acknowledged. Our thanks are also due to Prof. C. W. Bert of the University of Oklahoma for many helpful discussions during the course of the research on bimodular-material plates and shells.

REFERENCES

1. C. W. Bert and S. K. Kincannon, Bending-extensional coupling in elliptic plates of orthotropic bimodulus material. *Developments in Mechanics*, Vol. 10, pp. 7-11. (Proc. 16th Midwestern Mechanics Conference), Kansas State University, Manhattan, KS (Sept. 1979).
2. J. N. Reddy and W. C. Chao, Finite-element analysis of laminated bimodulus composite-material plates. *Comput. Structures* 12, 245-251 (1980).
3. C. W. Bert, J. N. Reddy, V. S. Reddy and W. C. Chao, Bending of thick rectangular plates laminated of bimodulus composite materials. *ALAA J.* 19, 1342-1349 (1981).
4. J. N. Reddy, C. W. Bert, Y. S. Hsu and V. S. Reddy, Thermal bending of thick rectangular plates of bimodulus composite materials. *J. Mech. Engng Sci.* 22, 297-304 (1980).

5. C. W. Bert, J. N. Reddy, W. C. Chao and V. S. Reddy, Vibration of thick rectangular plates of bimodulus composite material. *J. Appl. Mech.* **48**, 371–376 (1981).
6. N. Kamiya, Large deflection of a different modulus circular plate. *J. Engng Materials Technology, Trans. ASME*, **97H**, 52–56 (1975).
7. N. Kamiya, An energy method applied to large elastic deflection of a thin plate of bimodulus material. *J. Structural Mech.* **3**, 317–329 (1975).
8. J. N. Reddy, A penalty-plate bending element for the analysis of laminated anisotropic composite plates. *Int. J. Num. Meth. Engng* **15**, 1187–1206 (1980).
9. C. W. Bert, Models for fibrous composites with different properties in tension and compression. *J. Engng Maths. Tech. Trans. ASME* **99H**, 344–349 (1977).
10. S. A. Ambartsyanyan, The axisymmetric problem of a circular cylindrical shell made of material with different stiffnesses in tension and compression. *Izvestiya Akademiyi Nauk SSSR, Mekhanika*, pp. 77–85, No. 4, 1965. English translation, National Technical Information Service Document AD-675312 (1967).
11. S. Timoshenko, Strength of materials—II: *Advanced Theory and Problems*, 2nd Edn. Princeton, New Jersey.
12. G. S. Shapiro, Deformation of bodies with different tensile and compressive strengths [stiffnesses]. *Mech. Solids* **1**, 85–86 (1966).
13. N. Kamiya, Transverse shear effect in a bimodulus plate. *Nuclear Engng Design* **32**, 351–357 (1975).
14. R. M. Jones and H. S. Morgan, Bending and extension of cross-ply laminates with different moduli in tension and compression. *Comput. Structures* **11**, 181–190 (1980).
15. Y. S. Hsu, J. N. Reddy, and C. W. Bert, Thermoelasticity of circular cylindrical shells laminated of bimodulus composite materials. *J. Thermal Stresses* **4**, 155–177 (1981).
16. J. N. Reddy and C. W. Bert, On the behavior of plates laminated of bimodulus composite materials. *ZAMM* **62**, 213–219 (1981).
17. J. N. Reddy, Transient response of laminated, bimodular-material, composite rectangular plates, Report VPI-E-81.28; Department of Engineering Science and Mechanics, Virginia Polytechnic Institute and State University, Blacksburg, VA 24061.
18. J. M. Whitney and N. J. Pagano, Shear deformation in heterogeneous anisotropic composite plates. *ASME-J. Appl. Mech.* **37**, 1031–1036 (1970).

APPENDIX I

Elements of stiffness matrix

$$[K] = \begin{bmatrix} [K^{11}] & [K^{12}] & [K^{13}] & [K^{14}] & [K^{15}] \\ [K^{21}] & [K^{22}] & [K^{23}] & [K^{24}] & [K^{25}] \\ [K^{31}] & [K^{32}] & [K^{33}] & [K^{34}] & [K^{35}] \\ [K^{41}] & [K^{42}] & [K^{43}] & [K^{44}] & [K^{45}] \\ [K^{51}] & [K^{52}] & [K^{53}] & [K^{54}] & [K^{55}] \end{bmatrix} \quad (A1)$$

The matrix coefficients $K_{ij}^{\alpha\beta}$ are given by

$$\begin{aligned} [K^{11}] &= A_{11}[S^{xx}] + A_{66}[S^{yy}], \\ [K^{12}] &= A_{12}[S^{xy}] + A_{66}[S^{xy}]^T = [K^{21}]^T, \\ [K^{13}] &= A_{11}[R_x^{xx}] + A_{12}[R_y^{xy}] + A_{66}([R_y^{xy}]^T + [R_x^{yy}]) = \frac{1}{2}[K^{31}]^T, \\ [K^{14}] &= B_{11}[S^{xx}] + B_{66}[S^{yy}] = [K^{41}]^T, \\ [K^{15}] &= B_{12}[S^{xy}] + B_{66}[S^{xy}]^T = [K^{51}]^T, \\ [K^{22}] &= A_{22}[S^{yy}] + A_{66}[S^{xx}], \\ [K^{23}] &= A_{12}[R_x^{xy}]^T + A_{22}[R_y^{yy}] + A_{66}([R_x^{xy}] + [R_y^{xx}]) = \frac{1}{2}[K^{32}]^T, \\ [K^{24}] &= B_{12}[S^{xy}]^T + B_{66}[S^{xy}] = [K^{42}]^T, \\ [K^{25}] &= B_{22}[S^{yy}] + B_{66}[S^{xx}] = [K^{52}]^T, \\ [K^{33}] &= A_{55}[S^{xx}] + A_{44}[S^{yy}], \\ [K^{34}] &= \frac{1}{2} \int_{R^e} \left[\bar{N}_1 \frac{\partial \phi_1}{\partial x} \frac{\partial \phi_1}{\partial x} + \bar{N}_6 \left(\frac{\partial \phi_1}{\partial x} \frac{\partial \phi_1}{\partial y} \right) + \bar{N}_2 \frac{\partial \phi_1}{\partial y} \frac{\partial \phi_1}{\partial y} \right] dx dy, \\ [K^{35}] &= A_{55}[S^{xx}] = [K^{43}]^T, \\ [K^{34}] &= B_{11}[R_x^{xx}] + B_{12}[R_y^{xy}]^T + B_{66}([R_x^{yy}] + [R_y^{xx}]) = 2[K^{43}]^T, \\ [K^{35}] &= A_{44}[S^{yy}] = [K^{53}]^T, \\ [K^{35}] &= B_{12}[R_x^{xy}] + B_{22}[R_y^{yy}] + B_{66}([R_x^{xy}]^T + [R_y^{xx}]) = 2[K^{53}]^T, \\ [K^{44}] &= D_{11}[S^{xx}] + D_{66}[S^{yy}] + A_{55}[S], \\ [K^{45}] &= D_{12}[S^{xy}] + D_{66}[S^{xy}]^T = [K^{54}]^T, \\ [K^{55}] &= D_{66}[S^{xx}] + D_{22}[S^{yy}] + A_{44}[S]. \end{aligned} \quad (A2)$$

where

$$\begin{aligned}
 S_{ij}^{\xi\eta} &= \int_{R^*} \frac{\partial\phi_i}{\partial\xi} \frac{\partial\phi_j}{\partial\eta} dx dy, \quad \xi, \eta = 0, x, y, \quad S_{ij}^{00} \equiv S_{ij}, \\
 R_{ij}^{\zeta\eta} &= \int_{R^*} \frac{1}{2} \left(\frac{\partial w}{\partial\zeta} \right) \frac{\partial\phi_i}{\partial\xi} \frac{\partial\phi_j}{\partial\eta} dx dy, \quad \zeta, \xi, \eta = 0, x, y, \\
 \bar{N}_1 &= A_{11} \left(\frac{\partial w}{\partial x} \right)^2 + A_{12} \left(\frac{\partial w}{\partial y} \right)^2 + 2A_{16} \frac{\partial w}{\partial x} \frac{\partial w}{\partial y}, \\
 \bar{N}_2 &= A_{12} \left(\frac{\partial w}{\partial x} \right)^2 + A_{22} \left(\frac{\partial w}{\partial y} \right)^2 + 2A_{26} \frac{\partial w}{\partial x} \frac{\partial w}{\partial y}, \\
 \bar{N}_6 &= A_{16} \left(\frac{\partial w}{\partial x} \right)^2 + A_{26} \left(\frac{\partial w}{\partial y} \right)^2 + 2A_{66} \frac{\partial w}{\partial x} \frac{\partial w}{\partial y}
 \end{aligned} \tag{A3}$$

Here A_{ij} , B_{ij} , and D_{ij} are the plate stiffnesses,

$$\begin{aligned}
 (A_{ij}, B_{ij}, D_{ij}) &= \int_{-h/2}^{h/2} (1, z, z^2) Q_{ijkl} dz \quad (i, j = 1, 2, 6) \\
 A_{ij} &= \int_{-h/2}^{h/2} Q_{ijkl} dz \quad (i, j = 4, 5)
 \end{aligned} \tag{A4}$$

where h is the total thickness of the plate, Q_{ijkl} denotes the plane-stress reduced stiffness (i, j refer to the position in the compliance matrix; k refers to the sign of the fiber-direction strain: $k = 1$, tensile and $k = 2$, compressive; and l refers to the layer number), ϵ_j and κ_j are the strains and curvatures associated with the displacements in (2.1), and k_i are the shear correction coefficients (see [2-5]).